Chemical Research in Toxicology

Article

Cite This: Chem. Res. Toxicol. 2019, 32, 2118−2124

pubs.acs.org/crt

Reactivity of N3-Methyl-2′-Deoxyadenosine in Nucleosome Core Particles

Kun Yang,[†] Huabing Sun,[†] Leah Lowder,[‡] Sridhar Varadarajan,*[,‡] and Marc M. Greenberg*[,†]

[†]Department of Chemistry, Johns Hopkins University, 3400 North Charles Street, Baltimore, Maryland 21218, United States

[‡]Department of Chemistry and Biochemistry, University of North Carolina Wilmington, 601 South College Road, Wilmington, North Carolina 28403, United States

Supporting Information

ABSTRACT: N3-Methyl-2′-deoxyadenosine (MdA) is the major dA methylation product in duplex DNA. MdA blocks DNA replication and undergoes depurination at significantly higher rates than the native nucleotide from which it is derived. Recent reports on the effects of the nucleosome core particle (NCP) environment on the reactivity of N7-methyl-2′-deoxyguanosine (MdG) inspired this investigation concerning the reactivity of MdA in NCPs. NCPs containing MdA at selected positions were produced using a strategy in which the minor groove binding Me-Lex molecule serves as a sequence specific methylating agent. Hydrolysis of the glycosidic bond in MdA to form abasic sites (AP) is suppressed in a NCP. Experiments using histone variants indicate that the proximal, highly basic N-terminal tails are partially responsible for the decreased depurination rate constant. MdA also forms cross-links with histone proteins. The levels of MdA-histone DNA−protein cross-links (DPC_{MdA}) decrease significantly over time and are replaced by those involving AP. The time dependent decrease in DPC_{MdA} is attributed to the reversibility of their formation and the relatively rapid rate of AP formation from MdA. Overall, MdA reactivity in NCPs qualitatively resembles that of MdG.

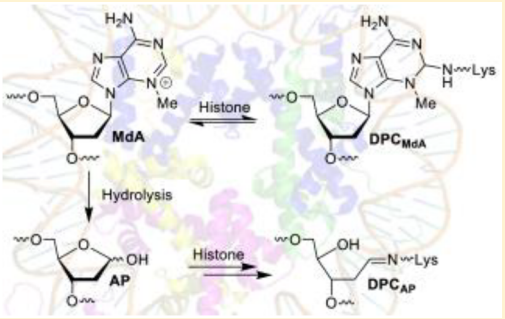

INTRODUCTION

DNA alkylation is a ubiquitous and biologically significant form of DNA damage.[1−3] Alkylated nucleotides can be mutagenic but are also a source of cytotoxicity induced by chemotherapeutic agents. Of the large variety of alkylating groups, methylation is the smallest and most common. Biologically important examples of methylating agents include current chemotherapeutic agents temozolomide (TMZ) and dacarbazine (DCZ) as well as *N*-methyl nitrosourea (MNU), dimethyl sulfate (DMS), and methylmethanesulfonate (MMS, Chart 1). N7-Methyl-2′-deoxyguanosine (MdG, 60−80%), N3-methyl-2′-deoxyadenosine (MdA, 10−20%), and O6-methyl-2′-deoxyguanosine (OmG, ≤5%) are the major DNA methylation products (Scheme 1). Although OmG is produced in the lowest chemical yield among the three products, the propensity of polymerases to misincorporate thymidine opposite it is believed to significantly contribute to the mutagenic and cytotoxic effects of methylating agents.[2] The correlation between cellular resistance to cytotoxic DNA methylating agents and levels of the OmG repair enzyme, O6-methylguanine-DNA methyltransferase, also attests to the biological significance of the lesion.[1] In contrast, other than being a source of abasic sites (AP), MdG was believed to have little biological consequence.[1,2] For instance, MdG was not believed to be cytotoxic or mutagenic.[4,5] However, recently, human DNA polymerase eta was found to bypass MdG with reduced fidelity.[6] In addition, we determined that histone proteins form reversible DNA−protein cross-links (DPCs) with the lesion.[7,8] DPC_{MdG} formation could significantly enhance the biological consequences of MdG, and their discovery fortuitously coincides with exciting discoveries concerning DPC repair in general.[9−13] The cellular lifetime of MdA is considerably shorter than that of MdG.[14] Unlike MdG, MdA blocks DNA replication and is cytotoxic.[15] MdA also undergoes depurination in free DNA more rapidly than does MdG. Furthermore, it has been shown that N3-methyladenine excision by base excision repair enzymes attenuates its toxicity.[16] Therefore, any alteration in the persistence of MdA in NCPs may play an important role in its

Chart 1. DNA Methylating Agents

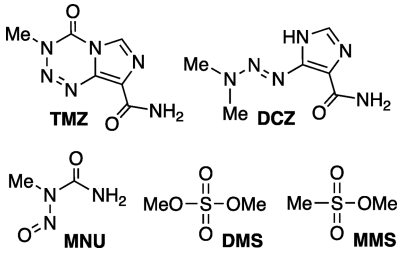

Received: July 24, 2019
Published: September 30, 2019

DOI: 10.1021/acs.chemrestox.9b00299
Chem. Res. Toxicol. 2019, 32, 2118−2124

Scheme 1. Formation and Reactivity of Methylated Purines

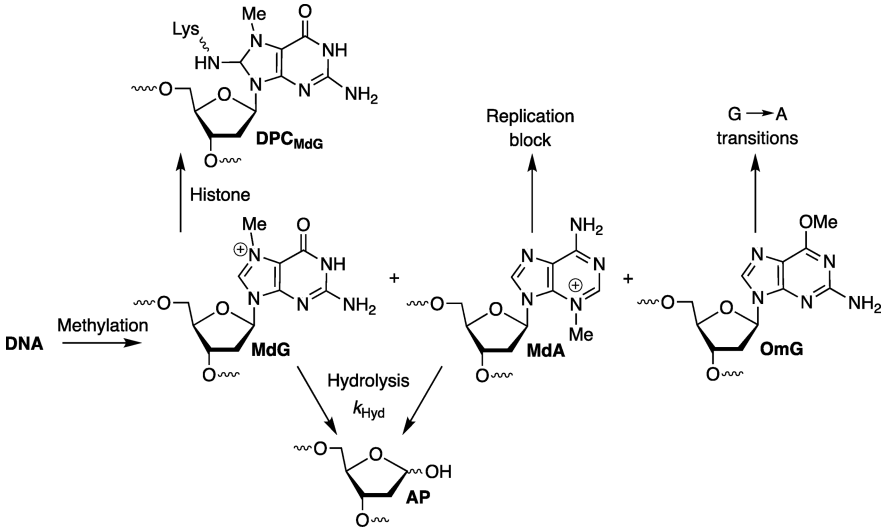

toxicity. Herein, we describe experiments using well-defined nucleosome core particles (NCPs) containing site-specific MdA to determine how the highly positively charged protein environment in chromatin affects the reactivity of this biologically significant DNA methylation product.

Alkylated purines undergo depurination >2000 times faster than the undamaged nucleotides.[3,17] The half-life of MdG in free DNA is 87−338 h.[7] The rate constants for depurination (k_{Hyd}, Scheme 1) of MdG are suppressed as much as almost 6-fold in a NCP compared to that in free DNA. The slowest k_{Hyd} determined within the NCP was at MdG_{123} (1×10^{-7} s^{-1}, $t_{1/2}$ = 1930 h). The magnitude of the decrease in k_{Hyd} correlates with the proximity of the lesion to the highly positively charged N-terminal histone tails. MdA undergoes depurination in free DNA even more rapidly than MdG. In addition, like MdG, methylation creates an electrophilic species that could react with nucleophilic residues within histone proteins to form DPCs. Consideration of the MdA electronic structure suggests that DPC formation will occur from histone attack in the minor groove, presumably at the C2-position, whereas MdG likely reacts at the C8-position within the major groove of duplex DNA (Scheme 1).

EXPERIMENTAL PROCEDURES

General Methods. Oligonucleotides used for polymerase chain reaction were purchased from Integrated DNA Technologies. Oligonucleotides for preparing 145-mer 601 DNA were synthesized on an Applied Biosystems Incorporated 394 oligonucleotide synthesizer. The oligonucleotide synthesis reagents were purchased from Glen Research (Sterling, VA). T4 polynucleotide kinase (PNK), terminal transferase, and proteinase K were from New England Biolabs. γ-^{32}P-ATP and α-^{32}P-cordycepin triphosphate were purchased from PerkinElmer. All experiments were performed in clear siliconized tubes from Bio Plas Incorporated. Quantification of radiolabeled oligonucleotides was done using a Molecular Dynamics Phosphorimager 840 equipped with ImageQuant TL software. 1-Methyl-4-(1-methyl-4-[3-(methoxysulfonyl)propanamido]pyrrole-2-carboxamido)pyrrole-2-carboxamido)propane (Me-Lex) was synthesized as previously described.[18]

Methylation of 601 DNA and NCPs by Me-Lex. Preparation of 601 DNA and NCPs with ^{32}P-labeling at the 5′-terminus of the top strand (1−145) or the 3′-terminus of the bottom strand (146−290) is described in the Supporting Information. Me-Lex (0.25 mg, 0.55 μmol) was dissolved in DMSO (55 μL) to a concentration of 10 mM, and then added to 5′- or 3′-^{32}P labeled free 601 DNA or NCPs (45 μL, 0.38 μM, ∼200,000 cpm) to a final concentration of 0.5 mM. The reaction mixture was incubated at 37 °C. An aliquot (15 μL) was taken after 0.5−1.5 h and stored on dry ice. All samples were phenol-chloroform extracted (equal volume), followed by ethanol precipitation (twice). The DNA was resuspended in 10 mM HEPES buffer (45 μL, pH 7.5) and heated at 90 °C for 15 min. The DNA was then ethanol precipitated, resuspended in piperidine solution (50 μL, 1 M), and heated (90 °C, 30 min). Piperidine was removed by evaporating to dryness in a speed vacuum. The products were resuspended in 95% formamide loading buffer (10 μL), and a portion of the sample (∼12,000 cpm) was analyzed by 10% denaturing PAGE. The gel (40 × 32 × 0.04 cm^3) was run at room temperature under limiting power (50 W) until the bromophenol blue migrated to the bottom.

Generation of 601 DNA Containing Site-Specifically Incorporated MdA. The 145-mer 601 DNA (200 pmol) and the scaffold (427 pmol, Figure S2) were combined in a buffer containing 10 mM phosphate (pH 7.2) and 100 mM NaCl. The mixture (∼1.1 mL) was heated at 90 °C for 30 s, followed by slowly cooling to room temperature. The hybridized DNA was mixed with 55 μL of a 10 mM Me-Lex solution in DMSO and incubated at 37 °C for 2 h (MdA_{58-59}) or 4 h ($MdA_{234-235}$). The methylated DNA was concentrated, and the unreacted Me-Lex and reaction by-products were removed by nine rounds of buffer exchange with a 10 mM HEPES buffer (pH 7.5) using a 10 kDa Amicon centrifugal filter at 4 °C. The methylated DNA product (50 μL, ∼200 pmol) was stored at −80 °C until further use.

Characterization of 601 DNA Containing Site-Specifically Incorporated MdA. The 145-mer MdA containing DNA was ^{32}P-labeled at the 5′-terminus (MdA_{58-59}) or 3′-terminus ($MdA_{234-235}$). For 5′-^{32}P labeling, the reaction mixture (20 μL) containing DNA (20 pmol), 1× PNK buffer (70 mM Tris−HCl, pH 7.6, 10 mM $MgCl_2$, 5 mM DTT), γ-^{32}P ATP (30 μCi), and T4 PNK (30 units) was incubated at room temperature for 3 h. For 3′-^{32}P labeling, the reaction mixture (20 μL) containing DNA (20 pmol), 1× terminal transferase buffer (20 mM Tris−acetate, pH 7.9, 50 mM CH_3COOK, 10 mM $Mg(CH_3COO)_2$), $CoCl_2$ (0.25 mM), α-^{32}P-cordycepin triphosphate (30 μCi), and terminal transferase (60 units) was incubated at room temperature for 3 h. Free γ-^{32}P-ATP and α-^{32}P-cordycepin triphosphate were removed using Sephadex G-50 resin (1 mL). To determine the extent of methylation at nucleotide resolution (methylation efficiency), the labeled DNA (130 fmol, ∼100,000 cpm) was diluted into 10 mM HEPES (50 μL, pH 7.5), heated (90 °C, 15 min), and then ethanol precipitated. The DNA pellet was resuspended in piperidine (50 μL, 1 M) and heated (90 °C, 30 min). To determine the AP content, the labeled DNA (130 fmol, ∼100,000 cpm) was subjected to hot piperidine treatment (50 μL, 1

DOI: 10.1021/acs.chemrestox.9b00299
Chem. Res. Toxicol. 2019, 32, 2118−2124

M, 90 °C, 30 min) without prior heating. Piperidine was removed by evaporating to dryness in a speed vacuum. The DNA was resuspended in 95% formamide (10 μL), and a portion of the sample (~10,000 cpm) was analyzed by 10% denaturing PAGE. The gel (40 × 32 × 0.04 cm^3) was run under limiting power (50 W) at room temperature until the xylene cyanol migrated to the bottom.

Reconstitution of NCPs Containing Site-Specifically Incorporated MdA. A mixture (10 μL) containing the complementary 145-mer (30 pmol), 10 mM phosphate buffer (pH 7.2), and 100 mM NaCl was heated at 90 °C for 1 min and immediately cooled on ice. The ^{32}P-labeled MdA containing DNA (20 μL, 20 pmol) was added and incubated at room temperature for 1 h. Salmon sperm DNA (20 μg, ~168 pmol of 185-bp DNA) and the hybridized 145-bp MdA containing DNA (2 pmol, ~4 million cpm) were combined in a siliconized tube to a final volume of 20 μL in the presence of 2 M NaCl and 0.1 mg/mL BSA. Histone octamer (1.2 equiv of total DNA) was added, and the mixture (22−30 μL) was incubated at 4 °C for 30 min before beginning a series of dilutions using the nucleosome reconstitution buffer (10 mM HEPES, pH 7.5, 1 mM EDTA, 0.1 mg/mL BSA) at 4 °C. Dilution #: volume of buffer added in μL, incubation time in minutes: 1: 24, 60; 2: 12, 60; 3: 12, 60; 4: 20, 30; 5: 20, 30; 6: 40, 30; 7: 100, 30; 8: 200, 30. After the final dilution (total volume ~450 μL), any precipitate was pelleted via a brief spin (1 min, 13,000*g*) at 4 °C. A small aliquot (5 μL, ~40,000 cpm) was removed, mixed with 3 μL of 40% sucrose, and analyzed by 6% native PAGE. The gel (10 × 8 × 0.15 cm^3) was run at 4 °C under limiting power (3 W) until the bromophenol blue band migrated to the bottom.

Determining AP Yields from NCPs Containing Site-Specifically Incorporated MdA. NCPs (140 μL, ~1 million cpm) containing site-specifically incorporated MdA were incubated at 37 °C. Aliquots (15 μL) were removed at appropriate times and stored at −80 °C until the final time point. To determine the amounts of AP, aliquots (10 μL) were treated with proteinase K (2.4 units) at room temperature for 30 min, followed by phenol−chloroform extraction (equal volume) and ethanol precipitation. The DNA was resuspended in piperidine (50 μL, 1 M) and heated (90 °C, 30 min). Piperidine was removed by evaporating to dryness in a speed vacuum. The samples were resuspended in 95% formamide loading buffer (10 μL), and a portion of the sample (~20,000 cpm) was analyzed by 10% denaturing PAGE. The gel (40 × 32 × 0.04 cm^3) was run at room temperature under limiting power (50 W) until the xylene cyanol migrated to the bottom. The normalized AP yield at each MdA (MdA_n) was calculated using eq 1. The rate constant for MdA hydrolysis (k_{Hyd}) was calculated by fitting the disappearance of MdA (1-normalized AP yield at MdA_n) to a first-order reaction.

$$\text{Normalized AP yield at } MdA_n = \frac{\%\ \text{cleaved DNA at } dA_n}{\text{methylation efficiency at } dA_n} \times 100\% \quad (1)$$

Determining DPC Yields from MdA and AP in NCPs Containing Site-Specifically Incorporated MdA. NCPs (120 μL/~850,000 cpm for 5.5 h of incubation, 25 μL/~180,000 cpm for 48 h of incubation) containing MdA_{58-59} or $MdA_{234-235}$ were incubated at 37 °C for 5.5 or 48 h, followed by 10% SDS PAGE analysis. The gel (20 × 16 × 0.1 cm^3) was run at 4 °C under limiting power (3 W) until the bromophenol blue migrated to the bottom. The DPC bands were cut out from the gel, crushed, and eluted overnight at 4 °C in a buffer (10 mM HEPES, pH 7.5, 200 mM NaCl, 1 mM EDTA) containing SDS (0.1%) and proteinase K (4 units). The gel particles were filtered using a polyprep column (BioRad). The filtrate was mixed with proteinase K (4 units) and incubated at room temperature for 10 min. Salmon sperm DNA (10 μg) was then added, followed by ethanol precipitation. The DNA samples (5000−10,000 cpm) were resuspended in H_2O (100 μL). To determine the total DPC yields (DPC_{Total}) from MdA and AP, the DNA samples (45 μL) were mixed with 100 mM HEPES buffer (5 μL, pH 7.5). The mixture was heated (90 °C, 15 min), followed by ethanol precipitation. The DNA samples were then subjected to hot piperidine treatment (1 M, 90 °C, 30 min). To determine the amount of DPC from AP (DPC_{AP}), an aliquot (45 μL) of the DNA samples isolated from the SDS PAGE was mixed with piperidine to a final concentration of 1 M and subjected to heating (90 °C, 30 min). Piperidine was removed by evaporating to dryness in a speed vacuum. DNA samples were resuspended in 95% formamide loading buffer (5 μL), and a portion of the sample (~1000 cpm) was analyzed by 10% denaturing PAGE. The gel (40 × 32 × 0.04 cm^3) was run at room temperature under limiting power (50 W) until the xylene cyanol migrated to the bottom. The yield of DPC from MdA (DPC_{MdA}) was calculated by subtracting the amount of DPC_{AP} from DPC_{Total}.

RESULTS AND DISCUSSION

Preparation of Nucleosome Core Particles Containing MdA. Neither MdG nor MdA can be incorporated into DNA using solid phase synthesis due to their chemical instability. MdG was successfully incorporated at specific positions using DNA polymerase and the corresponding deoxyribonucleotide triphosphate.[7] However, polymerase incorporation of MdA using the corresponding deoxyribonucleotide triphosphate was impractical due to the difficulty in synthesizing 3-methyl-2′-deoxyadenosine and its faster depurination than that of MdG.[19] Random incorporation of MdA by treating NCPs with a methylating agent (e.g., methylmethanesulfonate) was also impractical because dG was the major modification site (Figure S3).

Consequently, we took advantage of the ability of the *N*-methylpyrrole carboxamide, Me-Lex, to selectively introduce MdA into DNA.[18,20,21] The Widom 601 sequence is a good one for reaction with Me-Lex because it contains multiple regions rich in dA−T base pairs that are favored binding sites for *N*-methylpyrrole carboxamides.[22] In free DNA, Me-Lex preferentially alkylated dA_{58} and dA_{59} in one strand and dA_{234} and dA_{235} in the complementary strand (Figure 1 and Figure S4). These nucleotides are part of the 5′-d(T_{56}TAAAA$_{61}$) sequence. Two other dA/T rich sequences are alkylated to a lesser extent. Alkylation was biased toward dA_{58} in the top strand when the NCP was reacted with Me-Lex (Figure S4).

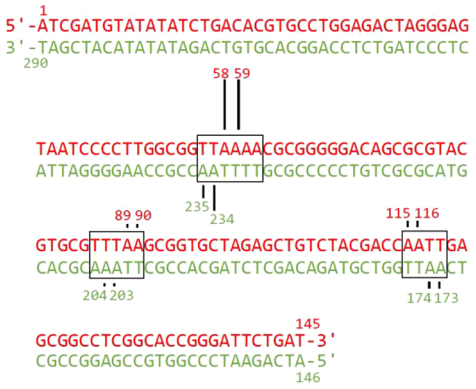

Figure 1. Me-Lex alkylation of free 601 DNA. The length of the lines is proportional to the amount of strand damage detected.

Detailed studies of MdA reactivity were carried out on NCPs in which the duplex region comprising 5′-d(T_{56}TAAAA$_{61}$) was alkylated. Selective methylation of this region was achieved by hybridizing one of the 145-mer strands with an oligonucleotide that hybridizes to this region (Scheme 2, Figures S5 and S6). The overall alkylation yield exceeded 60% at dA_{58} and dA_{59} and was ~50% at dA_{234} and dA_{235} in the complementary strand. The ratio of MdA_{59}:MdA_{58} or

DOI: 10.1021/acs.chemrestox.9b00299
Chem. Res. Toxicol. 2019, 32, 2118−2124

Scheme 2. Selective Introduction of MdA into DNA Using Me-Lex

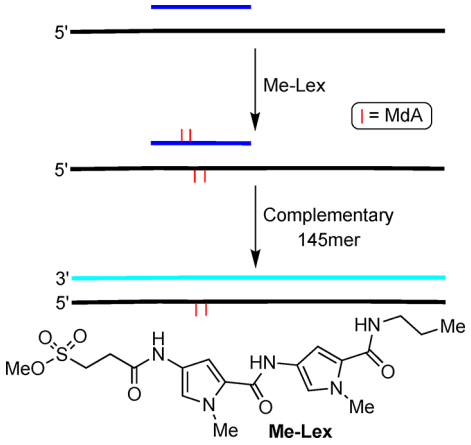

MdA_{234}:MdA_{235} did not change as a function of Me-Lex concentration or reaction time (Figures S5 and S6), indicating that each strand was alkylated only once. The 145-mer DNA was then ^{32}P-labeled at the 5′-terminus for the strand containing MdA_{58} and MdA_{59} (top strand) or at the 3′-terminus for the strand containing MdA_{234} and MdA_{235} (bottom strand). The ^{32}P-labeled DNA was hybridized with its complement, and the NCPs were reconstituted using refolded octamers comprised of recombinantly purified *Xenopus laevis* histone proteins that were expressed in *E. coli* (Figures S9 and S10). Approximately 5% of MdA was converted to AP during the entire DNA and NCP preparation process. The correct positioning of the DNA wrapping on octamer was confirmed by DNase I digestion (Figures S9 and S10). NCPs with a reconstitution efficiency larger than 93% were used for the experiments.

N3-Methyl-2′-deoxyadenosine Depurination. The rate constants for hydrolysis (k_{Hyd}, Scheme 1) were determined by measuring the amount of AP present as a function of time and normalizing for the MdA level at a particular position (Tables 1–4). AP levels were determined by taking advantage of the observation that hot piperidine treatment did not cleave DNA at MdA (Scheme 3, Figure S7). Consequently, direct hot piperidine treatment of DNA following proteinase K digestion selectively cleaves the DNA at AP sites, facilitating their quantitation following denaturing PAGE analysis, whereas the same process following heating yields strand scission at MdA and AP sites. Of the four positions at which depurination was examined, k_{Hyd} in free DNA ranged between 8×10^{-6} and 10.7×10^{-6} s^{-1} at three sites. MdA_{59} depurinates approximately 2–2.5 times faster than the other positions in free DNA. Hydrolysis of MdA was suppressed at all four positions within wild type NCPs. However, MdA_{59}, the most reactive alkylation site in free DNA, was affected the least within NCPs. The half-life for MdA_{59} depurination in the NCP was 1.9-fold longer than that in free DNA. In contrast, the relative half-lives (rel. $t_{1/2} = t_{1/2}$(NCP)/$t_{1/2}$(free DNA)) for MdA depurination at the other three positions ranged from 2.9 to 3.6.

The NCP effect on MdA depurination at these three positions is very similar to the effect on MdG_{89} (rel. $t_{1/2} = 2.9$) but significantly smaller than that on MdG_{123} (rel. $t_{1/2} = 5.7$).[7] Experiments with histone variants revealed that the proximal histone H2B N-terminal tail contributes significantly to the suppression of k_{Hyd} at MdG_{123}. MdG_{89} and the MdA positions

Table 1. MdA_{58} Depurination Kinetics as a Function of Environment

substrate	k_{Hyd} ($\times 10^{-6}$ s^{-1})	$t_{1/2}$ (h)	rel. $t_{1/2}$[c]
free DNA[b]	8.0 ± 1.1	24.4 ± 3.3	
WT[b]	2.2 ± 0.1	86.7 ± 3.2	3.6 ± 0.1
H3 Del.[b]	2.3 ± 0.5	84.7 ± 17.2	3.5 ± 0.9
H4 Del.[b]	2.9 ± 0.1	67.3 ± 0.1	2.8 ± 0.4
H3, H4 Del.[a]	3.1 ± 0.3	61.9 ± 6.8	2.5 ± 0.4

[a]Data are the average ± std. dev. of three replicates. [b]Data are the average ± std. dev. of two experiments each consisting of three replicates. [c]Rel. $t_{1/2} = t_{1/2}$(NCP)/$t_{1/2}$(free DNA).

Table 2. MdA_{59} Depurination Kinetics as a Function of Environment

substrate[a]	k_{Hyd} ($\times 10^{-6}$ s^{-1})	$t_{1/2}$ (h)	rel. $t_{1/2}$[b]
free DNA	20.4 ± 1.3	9.5 ± 0.6	
WT	10.7 ± 0.3	18.0 ± 0.5	1.9 ± 0.1
H3 Del.	10.8 ± 1.2	18.0 ± 1.9	1.9 ± 0.2
H4 Del.	13.0 ± 0.8	14.8 ± 1.0	1.6 ± 0.1
H3, H4 Del.	13.4 ± 2.8	14.4 ± 2.4	1.5 ± 0.3

[a]Data are the average ± std. dev. of three replicates. [b]Rel. $t_{1/2} = t_{1/2}$(NCP)/$t_{1/2}$(free DNA).

Table 3. MdA_{234} Depurination Kinetics as a Function of Environment

substrate[a]	k_{Hyd} ($\times 10^{-6}$ s^{-1})	$t_{1/2}$ (h)	rel. $t_{1/2}$[b]
free DNA	8.5 ± 0.4	22.6 ± 1.1	
WT	2.8 ± 0.2	68.7 ± 4.9	3.0 ± 0.3
H3 Del.	3.0 ± 0.7	66.2 ± 15.6	2.9 ± 0.7
H4 Del.	4.1 ± 0.2	47.5 ± 2.6	2.1 ± 0.2
H3, H4 Del.	3.8 ± 0.1	50.6 ± 1.3	2.2 ± 0.1

[a]Data are the average ± std. dev. of three replicates. [b]Rel. $t_{1/2} = t_{1/2}$(NCP)/$t_{1/2}$(free DNA).

Table 4. MdA_{235} Depurination Kinetics as a Function of Environment

substrate[a]	k_{Hyd} ($\times 10^{-6}$ s^{-1})	$t_{1/2}$ (h)	rel. $t_{1/2}$[b]
free DNA	10.7 ± 2.6	18.8 ± 4.9	
WT	3.0 ± 0.1	53.9 ± 2.5	2.9 ± 0.8
H3 Del.	4.8 ± 0.8	41.0 ± 7.0	2.2 ± 0.7
H4 Del.	6.2 ± 0.4	31.1 ± 2.1	1.6 ± 0.4
H3, H4 Del.	6.5 ± 1.1	29.1 ± 5.1	1.5 ± 0.5

[a]Data are the average ± std. dev. of three replicates. [b]Rel. $t_{1/2} = t_{1/2}$(NCP)/$t_{1/2}$(free DNA).

Scheme 3. Distinguishing MdA from AP

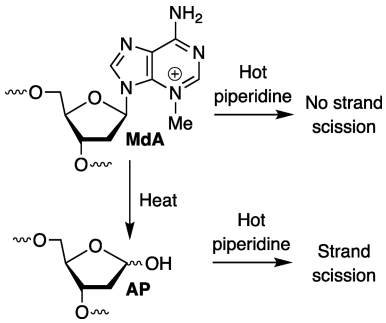

DOI: 10.1021/acs.chemrestox.9b00299
Chem. Res. Toxicol. 2019, 32, 2118–2124

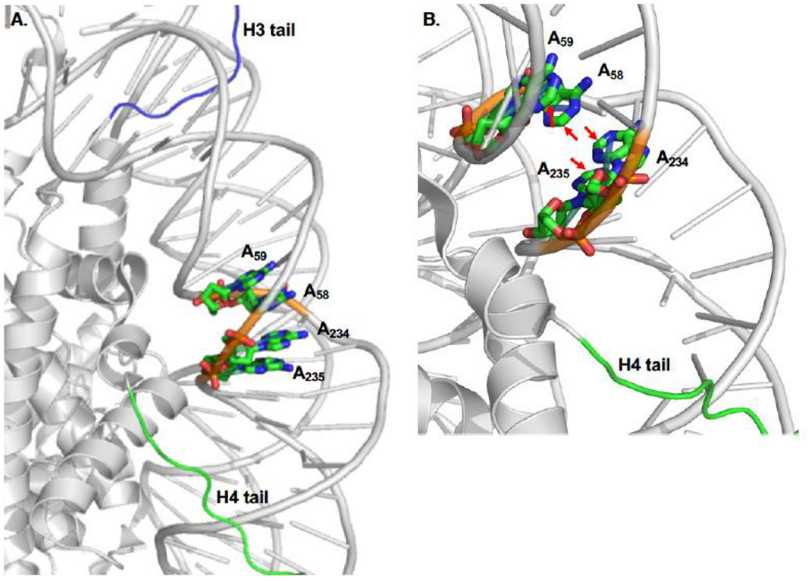

Figure 2. Nucleosome core particle structure in the vicinity of MdA_{58}, MdA_{59}, MdA_{234}, and MdA_{235}. (A) Major region damaged by Me-Lex showing histone H3 (blue) and H4 (green) N-terminal tails. (B) Zoomed in region showing C2-positions (red arrows) of alkylated dAs. The structure is generated by superimposing two NCP structures (pdb: 1kx5 and 3lz0).

Scheme 4. Distinguishing DPCs Formed from MdA and AP

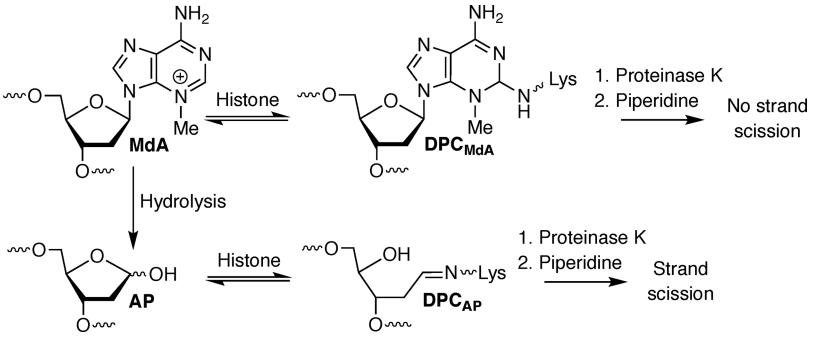

examined here are proximal to the histone H3 and H4 N-terminal tails (Figure 2). A molecular model based upon superimposed X-ray crystal structures of NCPs (pdb: 1kx5 and 3lz0) indicates that this histone H4 tail can interact with the minor groove in the vicinity of all four MdA molecules.[23,24] This flexible portion of the protein also appears to be able to interact with the major groove in which MdA_{234} and MdA_{235} are located. In contrast, the histone H3 tail, which protrudes from the core between the two DNA gyres in the NCP must traverse the DNA backbone to access the minor groove containing the methylated dA's. The major groove containing MdA_{58} and MdA_{59} is also relatively inaccessible to the histone H3 tail. However, the major groove in which MdA_{234} and MdA_{235} are positioned is in closer juxtaposition to the histone H3 tail.

These qualitative interpretations are largely borne out in kinetic studies involving NCPs containing histone variants. Deleting the 42 N-terminal amino acids from histone H3 has little if any effect on k_{Hyd} of MdA_{58}, MdA_{59}, or MdA_{234} (Tables 1−3). However, rel. $t_{1/2}$ of MdA_{235} is reduced from 2.9 to 2.2 when the histone H3 N-terminal tail is deleted. Deleting the histone H4 N-terminal tail increases k_{Hyd} at every MdA position. At one position, MdA_{58}, there is a small synergistic effect from deleting the N-terminal tails of histones H3 and H4 (Table 1).

Overall, the hydrolysis of MdA is similar to that of MdG in that it is significantly inhibited in a NCP. In addition, the proximal histone tail(s) has a similar effect on MdA depurination to that on the same reaction by MdG. It is also notable that the tails are not solely responsible for suppressing MdA hydrolysis in the NCPs relative to free DNA. This too was observed in experiments on MdG.

DNA−Protein Cross-Links at Positions Where N3-Methyl-2′-deoxyadenosine Is Incorporated. Inspired by the reversible DPC formation between MdG and histone proteins in NCPs, we examined whether MdA formed comparable products.[7] Detecting DPCs by SDS PAGE is straightforward. Determination of their origin is more complicated because the AP sites formed upon depurination form transient DPCs.[8,25,26] DPCs between histones and AP (DPC_{AP}) or MdA (DPC_{MdA}) are distinguishable by taking advantage of the facile cleavage of the DNA in the former, whereas the DNA in DPC_{MdA} is uncleaved when subjected to alkaline conditions (Scheme 4). In practice, the DPCs are isolated via SDS PAGE and the proteins are enzymatically degraded. The DNA is then subjected to alkaline conditions and analyzed by denaturing PAGE. Uncleaved and cleaved DNA are attributed to DPC_{MdA} and DPC_{AP}, respectively.

The DPC_{Total} (based upon the levels of MdA) at the respective alkylated positions ranged from approximately 3 to

DOI: 10.1021/acs.chemrestox.9b00299
Chem. Res. Toxicol. 2019, 32, 2118−2124

5% after incubating at 37 °C for 5.5 h but increased to as much as ∼22% upon incubation for 48 h (Table 5). The DPC yields

Table 5. DNA−Protein Cross-Link Yields as a Function of Incubation Time

	DPC_{Total} yield[a] (%)	
position	5.5 h	48 h
MdA_{58}	3.2 ± 0.3	17.8 ± 1.2
MdA_{59}	3.7 ± 0.4	22.2 ± 2.5
MdA_{234}	4.8 ± 0.7	19.5 ± 2.2
MdA_{235}	4.4 ± 0.6	17.2 ± 4.5

[a]Data are the average ± std. dev. of three replicates.

are considerably higher than what was observed in NCPs containing MdG.[7] DPCs were not detected when the NCPs containing MdA were comprised of histone H4 tail deletion variants, indicating that this protein is solely responsible for cross-link formation (Figure S13). In addition, the fraction of DPCs resulting from reaction with MdA (DPC_{MdA}) decreased at all positions over time (Figure 3). For instance, after incubating NCPs containing MdA_{58} and MdA_{59} for 5.5 h, DPC_{MdA} accounted for ∼42 and ∼28% of the DPCs, respectively. However, the contribution of DPC_{AP} in these NCPs to DPCs rose to more than 92% after 48 h (Figure 3A,B). The contribution of DPC_{MdA} to DPC formation was even smaller when the alkylated purines were present in the complementary strand (Figure 3C,D). After 48 h, more than 97% of the DPCs originating from methylation of dA_{234} and dA_{235} were attributable to AP lesions at these positions.

In general, the fraction of DPC_{MdA} is considerably smaller at all times than that of DPC_{MdG}.[7] This could be attributed to the irreversible nature of the depurination reaction and the significantly greater k_{Hyd} for MdA. Although DPC formation from AP, MdA, and MdG is reversible, depurination eliminates the possibility that the methylated nucleotide can contribute to this product family. Hence, the higher rate constants for MdA depurination reduce its contribution to DPC_{MdA} compared to the longer lived MdG. It is also possible that the C2-position of MdA, the presumed site of nucleophilic attack, which lies in the relatively narrow minor groove, may be less accessible to the histone tail(s). It is not clear from these experiments why MdA_{58} and MdA_{59} form DPC_{MdA} more readily than the methylated nucleotides on the complementary strand. There is no correlation between k_{Hyd} and DPC_{MdA} yields. For instance, the rate constants for depurination of MdA_{234} and MdA_{235} are very similar to that of MdA_{58}, yet DPC_{MdA} accounts for a much higher fraction of DPCs at the latter site. The absence of a correlation between k_{Hyd} and DPC yield is also evident at position 59. Hydrolysis at MdA_{59} is faster than that at the other three examined positions. However, it produces higher yields of DPC_{MdA} than do MdA_{234} and MdA_{235}. In addition, inspection of the NCP X-ray structure (Figure 2) does not suggest that the C2-positions of MdA_{58} and MdA_{59} are more accessible to the N-terminal histone H4 tail than MdA_{234} and MdA_{235}. One possibility is that the reversion rate constant for DPC_{MdA} involving MdA_{234} and MdA_{235} may be greater. However, we were unable to probe this possibility due to the heterogeneity of the DPC_{total} and low yields of DPC_{MdA}.

SUMMARY

N3-Methyl-2′-deoxyadenosine is recognized to be a block to DNA replication and a source of abasic sites. Recent studies on the reactivity of closely related N7-methyl-2′-deoxyguanosine in nucleosome core particles prompted this investigation.[7] MdA reactivity in NCPs parallels that of MdG. Specifically, the rate constant for MdA depurination is smaller in NCPs than in free DNA. The relative reduction is comparable to that observed for MdG in the same general region of the NCP. The proximal N-terminal histone H4 tail is a significant contributor to the observed suppression of depurination. However, the highly positively charged octameric core also plays a role in decreasing the rate constants for hydrolysis. MdA yields considerable amounts of DNA−protein cross-links. Although they are produced reversibly, this is to our knowledge the first evidence for the formation of DPCs between MdA and histone proteins. Unlike MdG, the vast majority of DPCs generated from MdA are ultimately between AP and the histone protein and not the alkylated nucleotide. The source of this difference is uncertain. Reversible formation of DPC_{MdA} and the more rapid depurination (k_{Hyd}) from MdA versus MdG may be one reason for the difference. In addition, the presumed need for nucleophilic attack of MdA by the histone tail(s) in the minor groove may also be a reason for the reduced levels of DPCs between MdA and histones compared to those involving MdG.

It is difficult to evaluate the role of decreased depurination of MdA in NCPs, as both MdA and AP are cytotoxic. DPCs are extremely deleterious because they block DNA replication and transcription. DPCs between histone proteins and MdG have been detected in cells treated with methylmethanesulfonate.[7] If DPC formation between histones and MdA in NCPs occurs in cells, they would also contribute to the cytotoxic effect of MdA even if formed in small amounts.

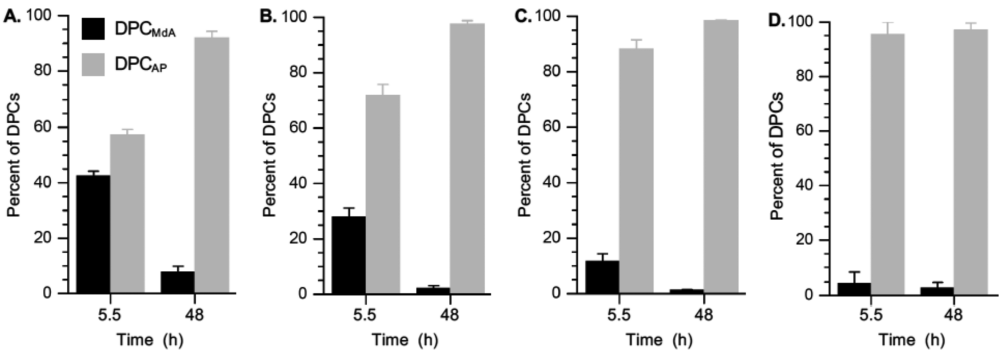

Figure 3. Distribution of DPCs as a function of time from (A) MdA_{58}, (B) MdA_{59}, (C) MdA_{234}, and (D) MdA_{235}.

DOI: 10.1021/acs.chemrestox.9b00299
Chem. Res. Toxicol. 2019, 32, 2118−2124

■ ASSOCIATED CONTENT

Supporting Information

The Supporting Information is available free of charge on the ACS Publications website at DOI: 10.1021/acs.chemrestox.9b00299.

Experimental methods for the 601 DNA preparation, NCP characterization, and sample autoradiograms (PDF)

■ AUTHOR INFORMATION

Corresponding Authors

*E-mail: varadarajans@uncw.edu.
*E-mail: mgreenberg@jhu.edu.

ORCID

Kun Yang: 0000-0001-5532-8810
Sridhar Varadarajan: 0000-0003-0986-9661
Marc M. Greenberg: 0000-0002-5786-6118

Funding

We are grateful for financial support from the National Institute of General Medical Sciences (GM-131736) to M.M.G. and from UNCW (Charles L. Cahill and CSURF Awards) to S.V.

Notes

The authors declare no competing financial interest.

■ ABBREVIATIONS

Me-Lex, 1-methyl-4-(1-methyl-4-[3-(methoxysulfonyl)-propanamido]pyrrole-2-carboxamido)pyrrole-2-carboxamido)-propane; MdA, N3-methyl-2′-deoxyadenosine; MdG, N7-methyl-2′-deoxyguanosine; OmG, O6-methyl-2′-deoxyguanosine; DPC, DNA−protein cross-link; DPC_{MdG}, DPC between MdG and histone protein; DPC_{MdA}, DPC between MdA and histone protein; DPC_{AP}, DPC between AP and histone protein; DPC_{Total}, total DPCs; AP, abasic site; NCP, nucleosome core particle

■ REFERENCES

(1) Bobola, M. S., Kolstoe, D. D., Blank, A., Chamberlain, M. C., and Silber, J. R. (2012) Repair of 3-methyladenine and abasic sites by base excision repair mediates glioblastoma resistance to Temozolomide. *Front. Oncol. 2*, 176.

(2) Fu, D., Calvo, J. A., and Samson, L. D. (2012) Balancing repair and tolerance of DNA damage caused by alkylating agents. *Nat. Rev. Cancer 12*, 104−120.

(3) Gates, K. S., Nooner, T., and Dutta, S. (2004) Biologically relevant chemical reactions of N7-alkylguanine residues in DNA. *Chem. Res. Toxicol. 17*, 839−856.

(4) Koag, M.-C., Kou, Y., Ouzon-Shubeita, H., and Lee, S. (2014) Transition-state destabilization reveals how human DNA polymerase *β* proceeds across the chemically unstable lesion N7-methylguanine. *Nucleic Acids Res. 42*, 8755−8766.

(5) Kou, Y., Koag, M. C., and Lee, S. (2015) N7 methylation alters hydrogen-bonding patterns of guanine in duplex DNA. *J. Am. Chem. Soc. 137*, 14067−14070.

(6) Njuma, O. J., Su, Y., and Guengerich, F. P. (2019) The abundant DNA adduct N7-methyl deoxyguanosine contributes to miscoding during replication by human DNA polymerase *η*. *J. Biol. Chem. 294*, 10253−10265.

(7) Yang, K., Park, D., Tretyakova, N. Y., and Greenberg, M. M. (2018) Histone tails decrease N7-methyl-2′-deoxyguanosine depurination and yield DNA−protein cross-links in nucleosome core particles and cells. *Proc. Natl. Acad. Sci. U. S. A. 115*, E11212−E11220.

(8) Yang, K., Prasse, C., and Greenberg, M. M. (2019) Effect of histone lysine methylation on DNA lesion reactivity in nucleosome core particles. *Chem. Res. Toxicol. 32*, 910−916.

(9) Mórocz, M., Zsigmond, E., Tóth, R., Enyedi, M. Z., Pintér, L., and Haracska, L. (2017) DNA-dependent protease activity of human spartan facilitates replication of DNA−protein crosslink-containing DNA. *Nucleic Acids Res. 45*, 3172−3188.

(10) Vaz, B., Popovic, M., Newman, J. A., Fielden, J., Aitkenhead, H., Halder, S., Singh, A. N., Vendrell, I., Fischer, R., Torrecilla, I., Drobnitzky, N., Freire, R., Amor, D. J., Lockhart, P. J., Kessler, B. M., McKenna, G. W., Gileadi, O., and Ramadan, K. (2016) Metalloprotease Sprtn/Dvc1 orchestrates replication-coupled DNA-protein crosslink repair. *Mol. Cell 64*, 704−719.

(11) Stingele, J., Bellelli, R., Alte, F., Hewitt, G., Sarek, G., Maslen, S. L., Tsutakawa, S. E., Borg, A., Kjær, S., Tainer, J. A., Skehel, J. M., Groll, M., and Boulton, S. J. (2016) Mechanism and regulation of DNA-protein crosslink repair by the DNA-dependent metalloprotease sprtn. *Mol. Cell 64*, 688−703.

(12) Lopez-Mosqueda, J., Maddi, K., Prgomet, S., Kalayil, S., Marinovic-Terzic, I., Terzic, J., and Dikic, I. (2016) Sprtn is a mammalian DNA-binding metalloprotease that resolves DNA-protein crosslinks. *eLife 5*, e21491.

(13) Larsen, N. B., Gao, A. O., Sparks, J. L., Gallina, I., Wu, R. A., Mann, M., Räschle, M., Walter, J. C., and Duxin, J. P. (2019) Replication-coupled DNA-protein crosslink repair by Sprtn and the proteasome in xenopus egg extracts. *Mol. Cell 73*, 574−588. e577

(14) Singer, B. (1979) N-Nitroso alkylating agents: Formation and persistence of alkyl derivatives in mammalian nucleic acids as contributing factors in carcinogenesis. *J. Nat. Cancer Inst. 62*, 1329−1339.

(15) Fronza, G., and Gold, B. (2004) The biological effects of N3-methyladenine. *J. Cell. Biochem. 91*, 250−257.

(16) Iyer, P., Srinivasan, A., Singh, S. K., Mascara, G. P., Zayitova, S., Sidone, B., E, F., Svilar, D., Sobol, R. W., Bobola, M. S., Silber, J. R., and Gold, B. (2013) Synthesis and characterization of DNA minor groove binding alkylating agents. *Chem. Res. Toxicol. 26*, 156−168.

(17) Lindahl, T., and Nyberg, B. (1972) Rate of depurination of native deoxyribonucleic acid. *Biochemistry 11*, 3610−3618.

(18) Zhang, Y., Chen, F. X., Mehta, P., and Gold, B. (1993) Groove- and sequence-selective alkylation of DNA by sulfonate esters tethered to lexitropsins. *Biochemistry 32*, 7954−7965.

(19) Fujii, T., Saito, T., and Nakasaka, T. (1989) Purines. XXXIV. 3-methyladenosine and 3-methyl-2′-deoxyadenosine: Their synthesis, glycosidic hydrolysis, and ring fission. *Chem. Pharm. Bull. 37*, 2601−2609.

(20) Encell, L., Shuker, D. E. G., Foiles, P. G., and Gold, B. (1996) The in vitro methylation of DNA by a minor groove binding methyl sulfonate ester. *Chem. Res. Toxicol. 9*, 563−567.

(21) Varadarajan, S., Shah, D., Dande, P., Settles, S., Chen, F.-X., Fronza, G., and Gold, B. (2003) DNA damage and cytotoxicity induced by minor groove binding methyl sulfonate esters. *Biochemistry 42*, 14318−14327.

(22) Dervan, P. B. (1986) Design of sequence-specific DNA-binding molecules. *Science 232*, 464−471.

(23) Luger, K., Rechsteiner, T. J., Flaus, A. J., Waye, M. M. Y., and Richmond, T. J. (1997) Characterization of nucleosome core particles containing histone proteins made in bacteria. *J. Mol. Biol. 272*, 301−311.

(24) Vasudevan, D., Chua, E. Y. D., and Davey, C. A. (2010) Crystal structures of nucleosome core particles containing the ′601′ strong positioning sequence. *J. Mol. Biol. 403*, 1−10.

(25) Sczepanski, J. T., Wong, R. S., McKnight, J. N., Bowman, G. D., and Greenberg, M. M. (2010) Rapid DNA-protein cross-linking and strand scission by an abasic site in a nucleosome core particle. *Proc. Natl. Acad. Sci. U. S. A. 107*, 22475−22480.

(26) Wang, R., Yang, K., Banerjee, S., and Greenberg, M. M. (2018) Rotational effects within nucleosome core particles on abasic site reactivity. *Biochemistry 57*, 3945−3952.

DOI: 10.1021/acs.chemrestox.9b00299
Chem. Res. Toxicol. 2019, 32, 2118−2124